# SUPERCONDUCTING CAVITY AND RF CONTROL LOOP MODEL FOR THE SPIRAL2 LINAC

F. Bouly*, LPSC, Université Grenoble-Alpes, CNRS/IN2P3, Grenoble, France
M. Di Giacomo, J.-F. Leyge, M. Tontayeva, GANIL, Caen, France

## Abstract

The SPIRAL2 superconducting linac has been successfully commissioned with protons in 2020. During the commissioning, a model of the cavity and its LLRF control loop has been developed. The model enables to have a better understanding of the system and was used to tune the PI(D) correctors for beam loading compensation. Here we review the development of such a tool, computed with MATLAB/Simulink to model transfer functions of : the RF and mechanical behaviors (Lorentz detuning) of the cavity, as well as all the elements that compose the RF control loop (digital LLRF, amplifier, transmission lines, etc.). A benchmarking of the model with measurements is presented.

## INTRODUCTION

A superconducting (SC) cavity model, with its associated control loops (Low level RF and Tuning system ) have been developed, by using Matlab/Simulink [1]. The aim of this model was to assess the technological feasibility of fast (∼ 100 ms) retuning of SC cavity for the operation of a CW (continuous wave) linac. This is a specific requirement for Accelerator Driven System (ADS) operation, where failure compensation is necessary to ensure a high reliability level of the machine [2, 3]. The model was also used to validate and adjust the incident coupling, as well as the performance requirements of the cold tuning system (CTS) actuators (motor, piezoelectric devices). It also enabled to carry out studies on 'intelligent' control of the CTS (Lorentz detuning compensation, microphonics damping, etc) [1, 4]. However, it had never been fully benchmarked on a cavity operating with beam. This has been achieved recently, during the commissioning and power ramp-up of the SPIRAL2 linac [5, 6]. We here give an overview of the model, present its benchmarking and the improvements : in particular for the digital LLRF model and the PI (proportional $K_p$, Integral $K_i$) controller.

## MODEL

The block diagram of Fig. 1 describes the global principle of the model. It consists in two loops :

- the LLRF feedback loop to control the phase and the amplitude of the accelerating voltage ($V_{cav}$),
- the feedback loop of the tuning system. The transfer function of the controller and the actuator acting on the cavity frequency detuning can be adjusted depending the simulation needs.
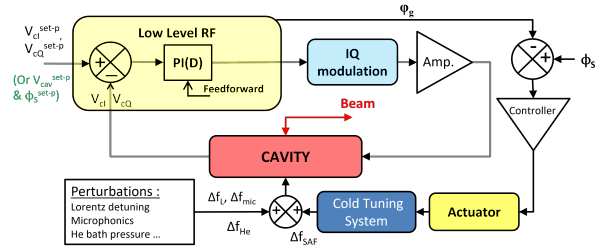
---

* frederic.bouly@lpsc.in2p3.fr

Figure 1: Model block diagram.

Computed in the Simulink environment, the main blocks of the RF feedback control loops are : the cavity, the LLRF, the IQ modulator and the RF power amplifier.

### Cavity Model

The cavity accelerating voltage, $V_{cav}$, is deduced by modelling the cavity as an RLC resonating circuit (cf. Fig. 2 equivalent model).
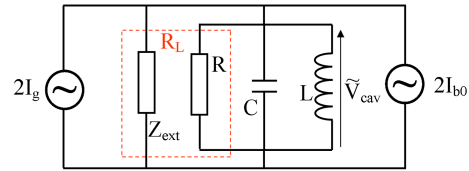


Figure 2: Equivalent circuit.

The RF power generator ($I_g$) and the beam ($I_{b0}$) are seen by the cavity as current generators [1, 7]. $R_L$ is the loaded shunt impedance, which is the sum of two parallel resistances: the external impedance (coupling) $Z_{ext}$, and the cavity resistance $R$. The loaded coupling is classically defined as :

$$\frac{1}{Q_L} = \frac{1}{Q_0} + \frac{1}{Q_i} + \frac{1}{Q_t} \tag{1}$$

with $Q_i$ the incident coupling from the power coupler, $Q_t$ the coupling from the pick-up antenna and $Q_0$ is the cavity quality factor. The digital LLRF system is treating I/Q (In phase / Quadrature) parts of the signal. It was chosen to use the same formalism to derive equations that define $V_{cav}$ evolution; and the associated Laplace transfer functions. As developed in [7], transient of the real part ($V_{cI}$) and imaginary part ($V_{cQ}$) of $V_{cav}$ can be written[1] :

$$\begin{cases} \dot{V}_{cI} = \frac{\omega_0(r/Q)}{4}\left(2I_{gI} + I_{bI}\right) - \frac{\omega_0}{2Q_L}\left[V_{cI} + V_{cQ}2Q_L\frac{\Delta\omega}{\omega_0}\right] \\ \dot{V}_{cQ} = \frac{\omega_0(r/Q)}{4}\left(2I_{gQ} + I_{bQ}\right) - \frac{\omega_0}{2Q_L}\left[V_{cQ} - V_{cI}2Q_L\frac{\Delta\omega}{\omega_0}\right] \end{cases} \tag{2}$$

---

[1] with the 'dot' notation $\dot{f} = \frac{df}{dt}$

with

$$I_{bI} = -2I_{b0} \qquad I_{bQ} = 0$$
$$I_{gI} = I_g \, \cos(\varphi_g) \qquad I_{gQ} = I_g \, \sin(\varphi_g) \qquad (3)$$
$$V_{cI} = V_{cav} \, \cos(\phi_s) \qquad V_{cQ} = V_{cav} \, \sin(\phi_s)$$

The 'linac definition' is used for the shunt impedance, $(r/Q) = V_{cav}^2/(\omega_0 W)$. $\omega_0$ is the RF angular frequency, and the cavity detuning, $\Delta f = f_0 - f_{cav}$ ($\Delta\omega = 2\pi\Delta f$), is calculated as :

$$\Delta f(t) = -\Delta f_L(t) - \Delta f_{mic}(t) - \Delta f_{He}(t) - \Delta f_{CTS}(t) \quad (4)$$

Microphonics ($\Delta f_{mic}$) and helium bath pressure ($\Delta f_{He}$) perturbations were not considered in this study but it can be implemented in the model. The tuning system ($\Delta f_{CTS}$) was considered as static, still transfer function of dynamic systems (e.g piezos) can be implemented [1, 4]. Lorentz detuning transients was considered with a first order equation [8] ($\tau_m$, mechanical constant and $k_L$, Lorentz factor ):

$$\tau_m \Delta \dot{f}_L(t) + \Delta f_L(t) = -k_L E_{acc}^2 \qquad (5)$$

### LLRF and PI controller

The LLRF block is a simplified model of the digital system. Delays and saturation are introduced as well as Zero Order Hold block to simulate the signal sampling. The LLRF sampling time is : $T_s = (4/5 * f_0)^{-1}$. Noise can also be simulated. Feedforward option was also introduced. When used, it basically consists in a reset of the PI blocks output to a given value - on each I and Q loop - when beam trigger is 'ON' [6]. Discrete PI controller from the Simulink library is used. The correction method used in the real LLRF system is a backward-Euler and it was implemented with discrete transfer function ('z-transform') :

$$H(z) = K_p + K_i.T e.\frac{z}{z-1} \qquad (6)$$

with $T_e = 4 * T_s$ , the sampling period of the controller. The controller model was carefully benchmarked to ensure that correctors coefficients ($K_p$ and $K_i.T_e$) match the values entered, by the operators, in the control system.

### Other subsystems

In this purpose, the effects of passive systems (waguide,cables, etc.) were taken into account. The attenuation (dephasing and delays when relevant) were crosschecked, measured and implemented in the model. The RF amplifier gain variation is also taken into account. $P_{ampli-out} = f(P_{in})$ was measured and implemented in the RF generator block. Similarly, the I/Q modulation $P_{I/Qmod} = f(V_{ILLRF}, V_{QLLRF})$ is also implemented and non-linearities are therefore considered.

## BENCHMARKING

The model was benchmarked with the first cavity from the B section of the SPIRAL2 linac [9]. Table 1 gives the main cavity and LLRF parameters. Figure 3 shows the beam loading effect and its compensation by the feedback LLRF loop (measurements and model). Measurements were carried out during the 16 kW power ramp-up with proton beam [5].

Table 1: Cavity and LLRF Parameters.

| Cavity parameters and set points | | | |
|---|---|---|---|
| $f_0$ | 88.0525 MHz | $(r/Q)$ | 515 $\Omega$ |
| $L_{acc}$ | 0.41 m | $k_L$ | 1.8 Hz/(MV/m) |
| $\tau_m$ | 1 ms | $Q_0$ | $2.5 \, 10^9$ |
| $Q_i$ | $9.9 \, 10^5$ | $Q_t$ | $1.8 \, 10^{11}$ |
| $E_{acc}$ | 6.449 MV/m | $\phi_s$ | -26° |
| $I_{b0}$ | 4.2 mA | $\Delta f$ | 7 Hz |
| **LLRF loop** | | | |
| Loop delay | 2 µs | $T_s$ | 14.2 ns |
| Max. RF Power | 23.4 kW | $T_e$ | 56.8 ns |
| I controller | | $K_{pI}$ | 50 |
| | | $K_{iI}$ | 0.1 |
| Q controller | | $K_{pQ}$ | 50 |
| | | $K_{iQ}$ | 0.1 |

Figure 3 shows a good agreement between the model and the measurements. The system behavior and the beam loading compensation is well reproduced. This tend to confirm the robustness of the model. It will enable to carry out PID tuning studies to anticipate the future LLRF settings, and this for each cavity of the linac. The phase difference - which is linked to the cavity detuning - is compared with the so called 'dpci' signal [6] of the SPIRAL2 LLRF system. The model also enables to calculate powers (reflected, transmitted, dissipated in cavity walls, etc), and in particular the RF power of the generator ($P_g$). The simulated evolution of $P_g$ is also matching quite well the measurements. Nevertheless, the fine calibration of the powers and of the detuning measurement are still in progress and should be confirmed. One can still conclude that the tendencies and order of magnitudes are well reproduced, especially for the accelerating field. For instance, the model was used during the commissioning to confirm that some correctors values was too low, and could be safely increased to optimise the beam loading compensation. It also enabled to confirm that feedforward is necessary to enhance the performances of the machine [6].

## FEEDBACK & FEEDFORWARD

As previously mentioned the model is used to carry out optimisation of the cavity control system: to tune the coefficients of the PI controller. Figure 4 shows another application example, where the integral coefficient of the I loop ($K_{iI}$) was identified as not properly tuned : ten times lower than the expected value. Once again the model is well reproducing the real system.

One other application of this model is to study the feedforward effect. Figure 5 illustrates how it can be used by comparing different tuning configurations: only feedback
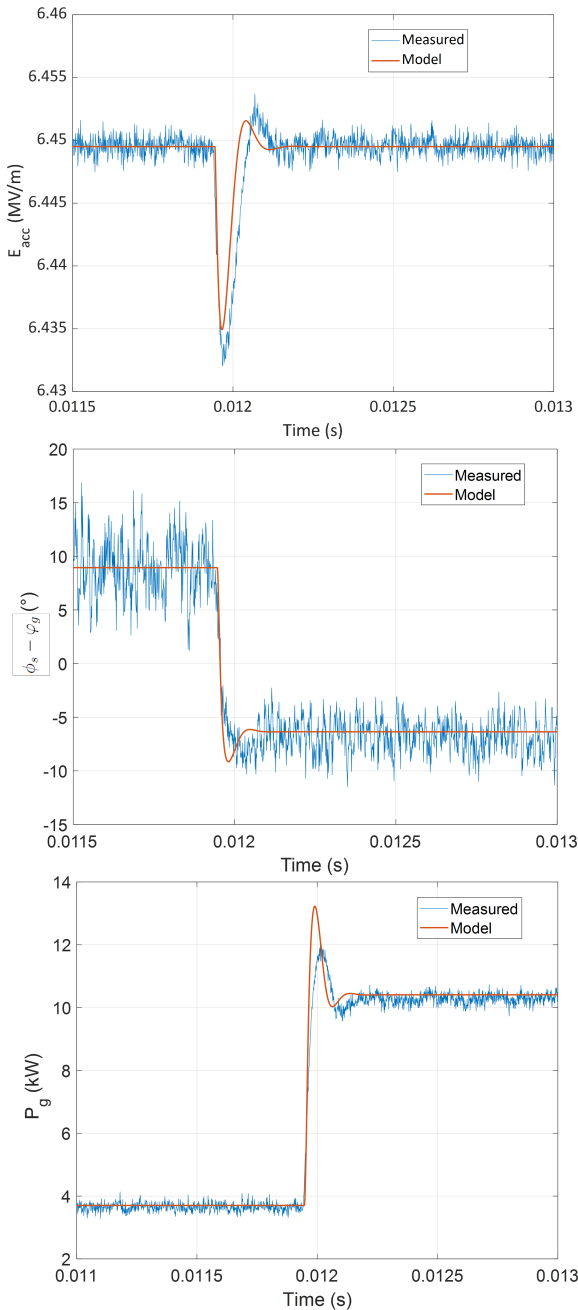
Figure 3: Accelerating Field, phase difference (detuning measurement) and RF power from amplifier at the beginning of a beam pulse.
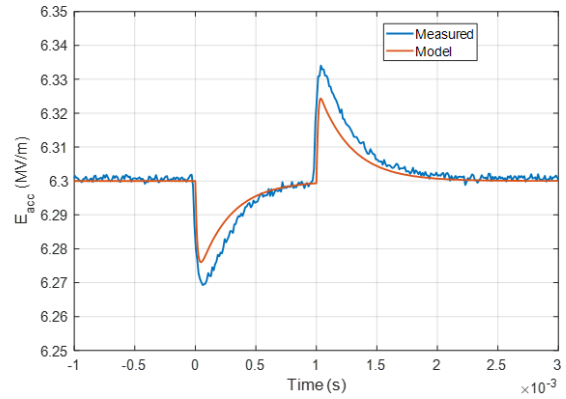


Figure 4: Beam loading effect in cavity 2 of the B section. $K_{pI} = K_{pQ} = 50$, $K_{iQ}.Te = 0.1$, but $K_{iI}.Te = 0.01$. $I_{b0} = 4.6$ mA with a pulse duration of 1 ms.
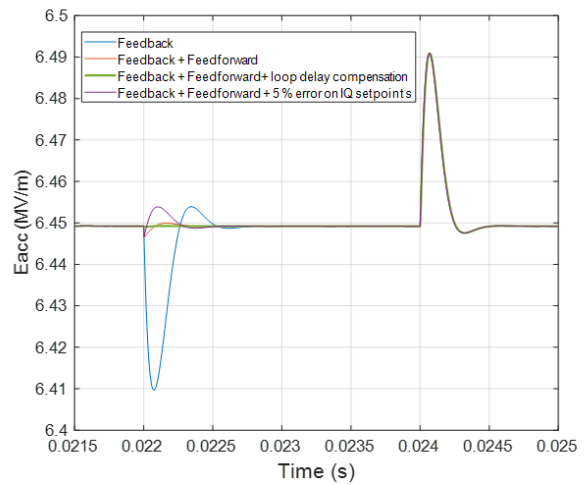


Figure 5: Example of feedback and feedforward effects . Here $K_{pI} = K_{pQ} = 15$ and $K_{iI}.Te = K_{iQ}.Te = 0.01$. $I_{b0} = 4.5$ mA with a pulse duration of 2 ms.

loop, feedback and feedforward triggered on the rising edge 'Beam ON', feedforward with loop delay compensation and feedforward with 5 % error on the $V_{cI}$ and $V_{cQ}$ set points. This example confirms that when not operating in CW - with low duty cycle but high beam loading - feedforward is necessary for the SPIRAL2 SC linac. And, as discussed in [6] delays compensation is a key point to enhanced the control of the beam loading during transients.

## CONCLUSION & PROSPECTS

A robust model of cavity and its associated feedback loops have been developed. This model can be adapted to different kind of cavity and tuning systems. It has been successfully benchmarked during the SPIRAL2 operation, especially for B cavities. The next steps will be to continue the fine tuning and benchmarking especially for section A of the SPIRAL2 linac. Studies to optimise the $K_p/K_i$ per loop (I and Q may have different corrections) will be carried out. In these purposes dedicated measurements are foreseen during next SPIRAL2 runs. The model can be used for other types of cavities e.g. Spokes for ADS projects [10–12], to study and provide control systems settings for fast retuning procedures (failure compensation [13]).

## REFERENCES

[1] F. Bouly, "Etude d'un module accélérateur supraconducteur et de ses systèmes de régulation pour le projet MYRRHA,"

Theses, Université Paris Sud - Paris XI, 2011. `https://tel.archives-ouvertes.fr/tel-00660392`

[2] F. Bouly, M. A. Baylac, A. Gatera, and D. Uriot, "Superconducting LINAC Design Upgrade in View of the 100 MeV MYRRHA Phase I," in *Proc. IPAC'19*, Melbourne, Australia, May 2019, pp. 837–840.
`doi:10.18429/JACoW-IPAC2019-MOPTS003`

[3] B. Yee-Rendon, "Overview of ADS Projects in the World," presented at LINAC'22, Liverpool, UK, Aug.-Sep. 2022, paper TU2AA1.

[4] I. Martin-Hoyo *et al.*, "Optimized Adaptive Control for the MYRRHA Linear Accelerator: Control System Design for a Superconducting Cavity in a Particle Accelerator," *IEEE Control Systems Magazine*, vol. 38, no. 2, pp. 44–79, 2018.
`doi:10.1109/MCS.2017.2786420`

[5] A. K. Orduz *et al.*, "Commissioning of a high power linac at GANIL: Beam power ramp-up," *Phys. Rev. Accel. Beams*, vol. 25, p. 060 101, 6 2022.
`doi:10.1103/PhysRevAccelBeams.25.060101`

[6] M. D. Giacomo *et al.*, "3 Operation Years of the Spiral2 Superconducting Linac - Rf Feedback," presented at LINAC'22, Liverpool, UK, Aug.-Sep. 2022, paper MOPOPA15.

[7] T. Schilcher, "Vector sum control of pulsed accelerating fields in Lorentz force detuned superconducting cavities," Ph.D. dissertation, DESY, 1998.

[8] A. Mosnier, "Control of SCRF Cavities in High Power Proton Linacs," in *Proc. EPAC'02*, Paris, France, Jun. 2002. `https://jacow.org/e02/papers/THXLA001.pdf`

[9] D. Longuevergne *et al.*, "Troubleshooting and Performances of Type-B Spiral2 Series Cryomodule," in *Proc. LINAC'14*, Geneva, Switzerland, Aug.-Sep. 2014, pp. 1037–1040.
`https://jacow.org/LINAC2014/papers/THPP078.pdf`

[10] C. Joly *et al.*, "MTCA.4-Based LLRF System Prototype Status for MYRRHA," presented at LINAC'22, Liverpool, UK, Aug.-Sep. 2022, paper THPOPA14.

[11] N. Gandolfo and D. L. Dréan, "Accelerated Lifetime Test of Spoke Cavity Cold Tuning Systems for Myrrha," presented at LINAC'22, Liverpool, UK, Aug.-Sep. 2022, paper TUPOJO23.

[12] C. Lhomme, F. Dieudegard, F. Chatelet, P. Duthil, and H. Saugnac, "An Approach for Component-Level Analysis of Cryogenic Process in Superconducting LINAC Cryomodules," presented at LINAC'22, Liverpool, UK, Aug.-Sep. 2022, paper TUPOGE04.

[13] A. Plaçais and F. Bouly, "Cavity Failure Compensation Strategies in Superconducting Linacs," presented at LINAC'22, Liverpool, UK, Aug.-Sep. 2022, paper TUPORI04.